

Iron Coordination Chemistry of Phenylpyruvate: An Unexpected κ^3 -Bridging Mode That Leads to Oxidative Cleavage of the C2–C3 Bond

Tapan K. Paine, Hui Zheng, and Lawrence Que, Jr.*

Department of Chemistry and Center for Metals in Biocatalysis, University of Minnesota, 207 Pleasant St. S.E., Minneapolis, Minnesota 55455

Received November 8, 2004

One mononuclear iron(II)–phenylpyruvate complex [Tp^{Ph2}Fe^{II}(PPH)] (1) of the tridentate face-capping Tp^{Ph2} ligand and two dinuclear iron(II)–phenylpyruvate enolate complexes [(6-Me₃-TPA)₂Fe^{II}₂(PP)]²⁺ (2) and [(6-Me₃-TPA)₂Fe^{II}₂(2-NO₂-PP)]²⁺ (3) of the tetradentate 6-Me₃-TPA ligand are reported to demonstrate two different binding modes of phenylpyruvate to the iron(II) centers. Phenylpyruvate binds in a κ^2 -(O,O) manner to the mononuclear Fe^{II}(Tp^{Ph2}) center of 1 but bridges in a κ^3 -(O,O,O) fashion to the two Fe^{II}(6-Me₃-TPA) centers of 2 and 3. Mononuclear complex 1 reacts with O₂ to undergo oxidative decarboxylation and *ortho*-hydroxylation of one of the aromatic rings of the Tp^{Ph2} ligand. In contrast, dinuclear complexes 2 and 3 react with O₂ to undergo oxidative cleavage of the C2–C3 bond of phenylpyruvate.

α -Ketoglutarate (α -KG)¹-dependent dioxygenases comprise a large class of non-heme iron enzymes that are essential for many biological functions, including post-translational modification of amino acid residues, DNA and RNA repair, and biosynthesis of antibiotics.^{2–4} Despite their diverse functions, all the enzymes in this class require the combination of a mononuclear iron(II) center, an α -keto acid, and dioxygen to effect two-electron oxidations of substrates concomitant with the oxidative decarboxylation of the keto acid. One member of this class, 4-hydroxyphenylpyruvate dioxygenase (HPPD), participates in tyrosine catabolism and catalyzes the conversion of 4-hydroxyphenylpyruvate to 2,5-dihydroxyphenylacetate in a reaction involving oxidative decarboxylation, side chain migration, and aromatic hydroxylation.⁵ It is one of a handful of enzymes in this class

where the α -keto acid function is incorporated into the substrate, unlike the more common variant in which the α -keto acid is a separate entity, typically α -ketoglutarate. Crystal structures of HPPD⁶ classify this enzyme among the superfamily of mononuclear non-heme iron(II)-dependent enzymes with a common 2-His-1-carboxylate facial triad motif.^{4,7} The uniqueness of HPPD among α -keto acid-dependent enzymes has led us to explore its iron coordination chemistry. While several iron(II)– α -keto acid model complexes have been reported,^{8–11} no iron(II)–phenylpyruvate model complex has been described thus far. We report herein a study of phenylpyruvate as ligand to iron(II) complexes of tridentate Tp^{Ph2} ligand¹² and tetradentate 6-Me₃-TPA ligand.¹³ Phenylpyruvate binds to FeTp^{Ph2} in the expected monoanionic bidentate mode; the complex reacts with O₂ and undergoes oxidative decarboxylation coupled with hydroxylation of one of the aromatic rings of the ligand. In contrast, phenylpyruvate binds to two Fe(6-Me₃-TPA) units in an unexpected tridentate dianionic bridging mode. This dinuclear complex also reacts with O₂ to undergo oxidative bond cleavage not of the C1–C2 bond but of the C2–C3 bond.

The reactions of Fe(ClO₄)₂·6H₂O, an N3 or N4 ligand, and phenylpyruvate in methanol yield iron(II) complexes with two different modes of binding of phenylpyruvate. The face-capping tridentate Tp^{Ph2} ligand forms mononuclear iron(II) complex [Tp^{Ph2}Fe^{II}(PPH)] (1)¹⁴ with a monoanionic phenylpyruvate, whereas the tetradentate 6-Me₃-TPA ligand

* Corresponding author. E-mail: que@chem.umn.edu.

- (1) Abbreviations: α -KG, α -ketoglutarate; Tp^{Ph2}, hydrotris(3,5-diphenylpyrazol-1-yl)borate; 6-Me₃-TPA, tris(6-methyl-2-pyridylmethyl)amine; PPH, phenylpyruvate; PP, enolate of phenylpyruvate; HPPD, 4-hydroxyphenylpyruvate dioxygenase; BF, benzoylformate; Tp^{Ph2*}, Tp^{Ph2} ligand hydroxylated at the *ortho* carbon of one 3-phenyl group.
- (2) Prescott, A. G.; Lloyd, M. D. *Nat. Prod. Rep.* **2000**, *17*, 367–383.
- (3) Solomon, E. I.; Decker, A.; Lehnert, N. *Proc. Natl. Acad. Sci. U.S.A.* **2003**, *100*, 3589–3594.
- (4) Costas, M.; Mehn, M. P.; Jensen, M. P.; Que, L., Jr. *Chem. Rev.* **2004**, *104*, 939–986.
- (5) Johnson-Winters, K.; Purpero, V. M.; Kavana, M.; Nelson, T.; Moran, G. R. *Biochemistry* **2003**, *42*, 2072–2080.

- (6) (a) Serre, L.; Sailland, A.; Sy, D.; Boudec, P.; Rolland, A.; Pebay-Peyroula, E.; Cohen-Addad, C. *Structure* **1999**, *7*, 977–988. (b) Brownlee, J. M.; Johnson-Winters, K.; Harrison, D. H. T.; Moran, G. R. *Biochemistry* **2004**, *43*, 6370–6377.
- (7) Hegg, E. L.; Que, L., Jr. *Eur. J. Biochem.* **1997**, *250*, 625–629.
- (8) Chiou, Y.-M.; Que, L., Jr. *J. Am. Chem. Soc.* **1995**, *117*, 3999–4013.
- (9) Ha, E. H.; Ho, R. Y. N.; Kisiel, J. F.; Valentine, J. S. *Inorg. Chem.* **1995**, *34*, 2265–2266.
- (10) Hikichi, S.; Ogihara, T.; Fujisawa, K.; Kitajima, N.; Akita, M.; Moro-Oka, Y. *Inorg. Chem.* **1997**, *36*, 4539–4547.
- (11) Mehn, M. P.; Fujisawa, K.; Hegg, E. L.; Que, L., Jr. *J. Am. Chem. Soc.* **2003**, *125*, 7828–7842.
- (12) Kitajima, N.; Fujisawa, K.; Fujimoto, C.; Moro-oka, Y.; Hashimoto, S.; Kitagawa, T.; Toriumi, K.; Tatsumi, K.; Nakamura, A. *J. Am. Chem. Soc.* **1992**, *114*, 1277–1291.
- (13) Zang, Y.; Kim, J.; Dong, Y.; Wilkinson, E. C.; Appelman, E. H.; Que, L., Jr. *J. Am. Chem. Soc.* **1997**, *119*, 4197–4205.

forms dinuclear iron(II) complexes $[(6\text{-Me}_3\text{-TPA})_2\text{Fe}^{\text{II}}_2(\text{PP})]^{2+}$ (**2**) and $[(6\text{-Me}_3\text{-TPA})_2\text{Fe}^{\text{II}}_2(2\text{-NO}_2\text{-PP})]^{2+}$ (**3**)¹⁵ with a dianionic phenylpyruvate moiety acting as a novel bridging ligand. Phenylpyruvate binds in a $\kappa^2\text{-(}O,O\text{)}$ manner to the mononuclear $\text{Fe}^{\text{II}}(\text{Tp}^{\text{Ph}_2})$ center of **1** but bridges in a $\kappa^3\text{-(}O,O,O\text{)}$ fashion to the two $\text{Fe}^{\text{II}}(6\text{-Me}_3\text{-TPA})$ centers of **2** and **3**.

The X-ray crystal structure of the neutral complex **1**¹⁶ reveals a five-coordinate iron(II) center with a monoanionic face-capping Tp^{Ph_2} and a bidentate phenylpyruvate anion comparable to those observed for corresponding five-coordinate benzoylformate and pyruvate complexes (Figure 1, top).¹¹ On the other hand, the X-ray crystal structure of the dicationic complex **2**¹⁷ reveals a diiron(II) complex with a dianionic phenylpyruvate (PP) acting as a bridging unit (Figure 1, bottom). In this structure, Fe1 has a distorted octahedral environment consisting of the tetradentate ligand and a bidentate PP dianion coordinated via O1 and O3. The Fe1–O1 distance of 2.219(3) Å is typical of an Fe(II)–carbonyl oxygen interaction, while the shorter Fe1–O3 distance of 1.970(3) Å is consistent with a negatively charged enolate oxygen. Unlike Fe1, the Fe2 ion is five-coordinate with the tetradentate ligand and the carboxylate oxygen from phenylpyruvate. The Fe2–O2 bond (1.988(3) Å) is 0.23 Å shorter than the corresponding Fe(II)–carbonyl Fe1–O1 bond, indicating a charge-localized carboxylate oxygen–Fe(II) interaction. Both Fe1 and Fe2 are coplanar with the PP dianion with an Fe1–O1–Fe2 angle of 175.48°. The C–O and C–C bond lengths of the α -keto acid moiety clearly indicate that phenylpyruvate has tautomered to its enolate form. The C44–O3 bond (1.322(6) Å), the longest among

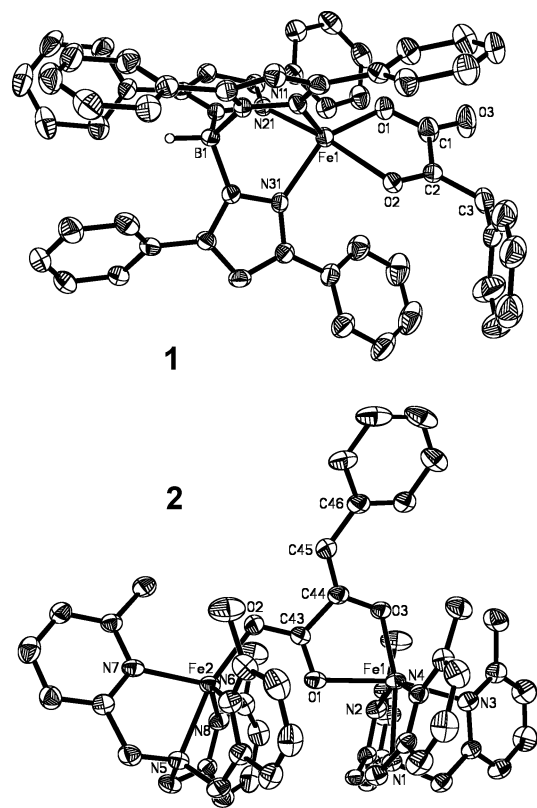


Figure 1. ORTEP plots of the neutral molecule $[\text{Tp}^{\text{Ph}_2}\text{Fe}(\text{PPH})]$ (**1**) and $[(6\text{-Me}_3\text{-TPA})_2\text{Fe}_2(\text{PP})]^{2+}$ (**2**), and the labeling scheme for selected atoms. All hydrogen atoms except that attached to boron atom on **1** have been omitted for clarity. Selected bond lengths [Å] and angles [deg] for **1**: Fe1–O1 1.965(4), Fe1–O2 2.270(4), Fe1–N11 2.083(3), Fe1–N31 2.083(3), Fe1–N21 2.145(3), O1–C1 1.288(8), O2–C2 1.232(7), C2–C3 1.487(7), C1–C2 1.527(8), O1–Fe1–N31 139.3(3), N21–Fe1–O2 177.8(3). Selected bond lengths [Å] and angles [deg] for **2**: Fe1–O1 2.219(3), Fe1–O3 1.970(3), Fe2–O2 1.988(3), Fe1–N1 2.201(4), Fe1–N4 2.253(4), Fe2–N5 2.192(4), Fe2–N6 2.229(4), C43–O1 1.259(5), C44–O3 1.322(6), C43–O2 1.282(6), C43–C44 1.509(6), C44–C45 1.343(6), O3–Fe1–N1 164.49(14), O1–Fe1–N3 164.06(12), O3–Fe2–N5 161.64(14), N8–Fe2–N6 136.63(15).

- (14) Complex **1**: Equimolar amounts (0.5 mmol) of KTp^{Ph_2} , sodium phenylpyruvate, and $\text{Fe}(\text{ClO}_4)_2 \cdot 6\text{H}_2\text{O}$ in 8 mL of MeOH were stirred under argon for 0.5 h. The solution was then concentrated to dryness, and the isolated orange solid was dissolved in CH_2Cl_2 . The resulting solution was filtered, and the filtrate was kept in an ether bath for slow vapor diffusion. An orange crystalline solid was formed overnight, which was then filtered and dried. Yield: 0.18 g (41%). Anal. Calcd for **1**·2 CH_2Cl_2 , $\text{C}_{56}\text{H}_{45}\text{BCl}_4\text{FeN}_6\text{O}_3$: C, 63.54; H, 4.29; N, 7.94. Found: C, 63.89; H, 4.35; N, 7.98.
- (15) Complex **2**-(**BPh**₄)₂: Equimolar amounts (0.5 mmol) of 6- $\text{Me}_3\text{-TPA}$, sodium phenylpyruvate, and $\text{Fe}(\text{ClO}_4)_2 \cdot 6\text{H}_2\text{O}$ in 8 mL of MeOH were stirred under argon for 2 h. The resulting solution was then treated with a methanolic solution of NaBPh_4 (0.5 mmol) to precipitate a yellow microcrystalline solid, which was isolated by filtration, washed with methanol, and dried. X-ray quality crystals were grown by vapor diffusion of ether into a dichloromethane solution of **2**. Yield: 0.30 g (76%). Anal. Calcd for **2**-(**BPh**₄)₂·0.5 CH_2Cl_2 , $\text{C}_{99.5}\text{H}_{95}\text{B}_2\text{ClFe}_2\text{N}_8\text{O}_3$: C, 73.79; H, 5.91; N, 6.92. Found: C, 74.19; H, 5.95; N, 6.96. Complex **3**-(**BPh**₄)₂: **3** was similarly obtained except that 2-nitrophenylpyruvic acid and triethylamine were used instead of sodium phenylpyruvate. Yield: 0.37 g (91%). Anal. Calcd for **3**-(**BPh**₄)₂·0.5 CH_2Cl_2 , $\text{C}_{99.5}\text{H}_{94}\text{B}_2\text{ClFe}_2\text{N}_9\text{O}_3$: C, 71.79; H, 5.69; N, 7.57. Found: C, 71.80; H, 5.66; N, 7.61.
- (16) Crystal data for **1**·2 CH_2Cl_2 : $\text{C}_{56}\text{H}_{45}\text{BCl}_4\text{FeN}_6\text{O}_3$, $M_f = 1058.44$, monoclinic, $a = 10.056(3)$ Å, $b = 37.072(9)$ Å, $c = 13.409(3)$ Å, $\alpha = 90^\circ$, $\beta = 90.223(4)^\circ$, $\gamma = 90^\circ$, $V = 4999(2)$ Å³, $T = 173(2)$ K, space group $P2_1/n$, $Z = 4$, 8797 independent reflections used for solution and refinement (SHELXL-97) by full-matrix least-squares on F^2 . The final full-matrix least-squares refinement converged to $R1 = 0.0555$ and $wR2 = 0.1249$ (F^2 , all data).
- (17) Crystal data for **2**-(**BPh**₄)₂· CH_2Cl_2 : $\text{C}_{100}\text{H}_{96}\text{B}_2\text{Cl}_2\text{Fe}_2\text{N}_8\text{O}_3$, $M_f = 1662.07$, triclinic, $a = 12.1918(18)$ Å, $b = 16.306(2)$ Å, $c = 22.117(3)$ Å, $\alpha = 89.414(3)^\circ$, $\beta = 78.086(3)^\circ$, $\gamma = 87.962(3)^\circ$, $V = 4299.5(11)$ Å³, $T = 173(2)$ K, space group $P1$, $Z = 2$, 15055 independent reflections used for solution and refinement (SHELXTL) by full-matrix least-squares on F^2 . The final full-matrix least-squares refinement converged to $R1 = 0.0720$ and $wR2 = 0.2179$ (F^2 , all data).

the three C–O bonds, is a C–O single bond derived from the enolate form of phenylpyruvate. The C44–C45 distance of 1.343(6) Å, significantly shorter than the C43–C44 distance of 1.509(6) Å, corresponds to a double bond.¹⁸ Complex **2** is the first example of a complex with a bridging phenylpyruvate dianion. The ESI mass spectra of **2** and **3** in MeCN show signals at m/z 469.2 and 491.6, respectively, with the expected isotope distribution pattern, indicating that the dimeric structures remain intact in solution.

The structures in Figure 1 show that phenylpyruvate can act as a monoanionic or a dianionic ligand. In the latter case, the phenylpyruvate dianion forms spontaneously, without requiring the addition of base. We attribute this result to the more Lewis acidic metal center of $\text{Fe}(6\text{-Me}_3\text{-TPA})^{2+}$ (vs $\text{Fe}(\text{Tp}^{\text{Ph}_2})^+$) that promotes enolization of the coordinated phenylpyruvate and stabilizes the dianionic bridging structure.

Mononuclear complex **1** is red-orange in benzene solution and reacts with O_2 at ambient temperature over the period

(18) Gatehouse, B. M.; O'Connor, M. J. *Acta Crystallogr.* **1976**, *B32*, 3145–3148.

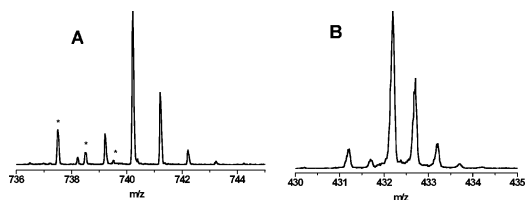


Figure 2. ESI-MS spectra of the oxidized products from **1** (A) and **2** (B) [asterisk-marked peaks are from the polypropyleneglycol internal standard].

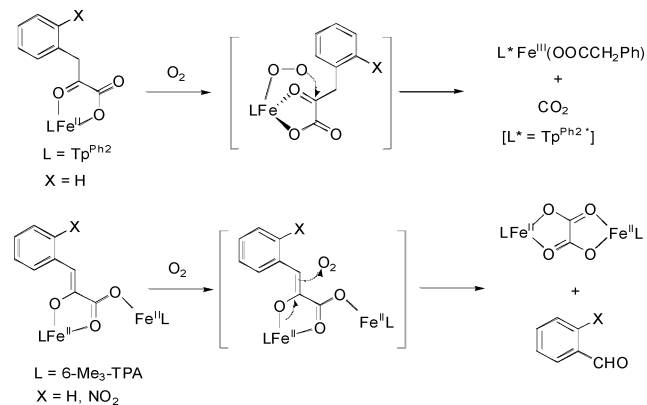
of an hour to generate a green species ($\lambda_{\max} = 650 \text{ nm}$), in which the *ortho* carbon of one 3-phenyl group has been hydroxylated. This iron(III) phenolate product is formulated as $[\text{Fe}^{\text{III}}(\text{Tp}^{\text{Ph}2*})(\text{O}_2\text{CCH}_2\text{Ph})]$ by spectroscopic comparison with a closely related iron(III) phenolate complex that has been structurally characterized.¹¹ Like $[\text{Fe}^{\text{III}}(\text{Tp}^{\text{Ph}2*})(\text{O}_2\text{CPh})]$, $[\text{Fe}^{\text{III}}(\text{Tp}^{\text{Ph}2*})(\text{O}_2\text{CCH}_2\text{Ph})]$ shows an intense signal at $g = 4.3$ in its EPR spectrum, typical of an iron(III) center in a rhombic environment, and a major ion at $m/z = 740.2$ in its ESI mass spectrum (Figure 2A), corresponding to $[\text{Fe}^{\text{III}}(\text{Tp}^{\text{Ph}2*})]^+$, with an isotope distribution pattern similar to that calculated for this fragment. A 50% yield can be estimated on the basis of the extinction coefficient reported for $[\text{Fe}^{\text{III}}(\text{Tp}^{\text{Ph}2*})(\text{O}_2\text{CPh})]$.¹¹ Thus, **1** is capable of oxygen activation and arene hydroxylation.

In contrast, **2** reacts with O_2 in MeCN at ambient temperature to afford a yellow solution over a period of an hour. The ESI mass spectrum of the yellow solution shows a peak at $m/z 432.2$ with an isotope distribution pattern indicative of a dication (Figure 2B). The observed m/z value matches that of $[(6\text{-Me}_3\text{-TPA})_2\text{Fe}^{\text{II}}_2(\mu\text{-oxalato})]^{2+}$ (**4**), which has been synthesized independently by self-assembly.¹⁹ Indeed, the ^1H NMR spectrum of synthesized **4** is identical to that of the yellow solution obtained after the oxidation of **2**. Complex **3** reacts as well with O_2 to give the same oxalate bridged iron(II) dimer, except that it reacts three times more slowly. The slow rate is consistent with the presence of a nitro substituent on the aromatic ring of the PP moiety in **3**, which makes it a poorer electron donor and thus relatively less reactive toward O_2 .

Further analyses of the reaction solutions after oxidations by GC and GC-MS revealed the presence of organic products benzaldehyde and 2-nitrobenzaldehyde after oxidations of **2** and **3**, respectively. The organic product was quantified by GC, and the yields of aldehydes were found to be in the range 40–50%. This clearly demonstrates the activation of O_2 by complexes **2** and **3** and subsequent cleavage of the PP C2–C3 bond to give oxalate and benzaldehydes (Scheme 1). The cleavage is the first of its kind observed thus far.

(19) Complex **4**-(ClO_4)₂: Equimolar amounts (0.25 mmol) of 6-Me₃-TPA, sodium oxalate and $\text{Fe}(\text{ClO}_4)_2 \cdot 6\text{H}_2\text{O}$ in 5 mL of MeOH were stirred under argon. The solution turned yellow immediately, and a yellow microcrystalline solid precipitated from the solution, which was isolated by filtration, washed with methanol, and dried. Yield: 0.11 g (85%). Anal. Calcd for **4**-(ClO_4)₂, $\text{C}_{44}\text{H}_{48}\text{B}_2\text{Cl}_2\text{Fe}_2\text{N}_8\text{O}_{12}$: C, 49.69; H, 4.55; N, 10.54. Found: C, 49.39; H, 4.75; N, 10.16.

Scheme 1. Reaction Scheme for the Oxidation of **1–3**



Because similar products are obtained, the C1–C2 oxidative cleavage observed for **1** must follow the mechanism proposed for analogous $[\text{Tp}^{\text{Ph}2}\text{Fe}^{\text{II}}(\text{BF})]$.¹¹ This mechanism consists of O_2 binding at the coordinatively unsaturated iron(II) center and subsequent attack of the incipient superoxide at the keto carbon of the α -keto acid. For **2** and **3**, C2–C3 oxidative cleavage must occur via a distinct pathway. Because of the coordinative saturation of Fe1 in **2** and **3**, we propose that O_2 directly attacks the electron-rich C3 atom of the dianionic enolized PP to set up C2–C3 cleavage. Thus, how the substrate is bound to the metal center affects the outcome of its reaction with O_2 .

In summary, we have isolated and characterized iron(II) complexes with two distinct phenylpyruvate binding modes that react with O_2 to undergo oxidative cleavage of a C–C bond. The C1–C2 cleavage reactivity of **1** mimics that of HPPD and α -KG-dependent enzymes. But unlike for HPPD, the arene hydroxylated is a phenyl ring on the $\text{Tp}^{\text{Ph}2}$ ligand, rather than the phenyl ring of the PPH ligand. The C2–C3 cleavage reactivity of **2** and **3**, on the other hand, is reminiscent of biodegradative non-heme iron enzymes such as the catechol dioxygenases⁴ and the β -diketone dioxygenases²⁰ that involve substrates with enolate functionalities. These results demonstrate the key role coordination chemistry can play in directing the course of an oxidative transformation.

Acknowledgment. This work was supported by the National Institutes of Health (GM-33162). We thank Dr. Victor G. Young, Jr., and William W. Brennessel of the University of Minnesota X-ray Crystallographic Laboratory for determining the crystal structures.

Supporting Information Available: Crystallographic data in CIF format. This material is available free of charge via the Internet at <http://pubs.acs.org>.

IC048427K

(20) Straganz, G. D.; Hofer, H.; Steiner, W.; Nidetzky, B. *J. Am. Chem. Soc.* **2004**, *126*, 12202–12203.